Table-top soft X-ray microscopy with a laser-induced plasma source based on a pulsed gas-jet

Matthias Müller, Tobias Mey, Jürgen Niemeyer, Maike Lorenz, and Klaus Mann

Citation: AIP Conference Proceedings **1764**, 030003 (2016); doi: 10.1063/1.4961137
View online: http://dx.doi.org/10.1063/1.4961137
View Table of Contents: http://scitation.aip.org/content/aip/proceeding/aipcp/1764?ver=pdfcov
Published by the AIP Publishing

Table-top Soft X-ray Microscopy with a Laser-induced Plasma Source Based on a Pulsed Gas-jet

Matthias Müller[1, a)] Tobias Mey[1], Jürgen Niemeyer[2], Maike Lorenz[3], and Klaus Mann[1]

[1]Laser-Laboratorium Göttingen e.V., Hans-Adolf-Krebs-Weg 1, D-37077 Göttingen, Germany
[2]Department für Nutzpflanzenwissenschaften, Georg-August-Universität Göttingen, Carl-Sprengel-Weg 1, D-37075 Göttingen, Germany
[3]Experimentelle Phykologie und Sammlung von Algenkulturen, Georg-August-Universität Göttingen, Nikolausberger Weg 18, D-37073 Göttingen, Germany

[a)]Corresponding author: matthias.mueller@llg-ev.de

Abstract. A table-top soft x-ray microscope based on a long-term stable and nearly debris-free laser plasma from a pulsed nitrogen gas jet target is presented. The microscope operates in the "water window" region at 2.88 nm wavelength. The emitted soft x-ray radiation is focused by an ellipsoidal condenser mirror into the object plane and a sample is imaged using a Fresnel zone plate onto a CCD camera. The spatial resolution of the microscope is about 50 nm demonstrated for a Siemens star test pattern.

INTRODUCTION

Transmission x-ray microscopy in the spectral range of the "water window" region ($\lambda = 2.3 - 4.4$ nm) is a powerful tool for the investigation of biological and mineralogical samples, including, e.g., tomographic studies of cryogenic cells [1-8] and spectromicroscopic analysis of soils due to the element-specific contrast [9]. Spatial resolutions of 10 nm have been achieved [10] making use of Fresnel zone plates as highly magnifying objectives. However, soft x-ray microscopy is almost exclusively performed at synchrotron sources providing the necessary high photon flux of short wavelength radiation.

To enable soft x-ray microscopy for everyday use without waiting times due to limited beam time at large-scale facilities, lab-scale sources based on gas discharge or laser-produced plasmas for soft x-ray microscopy have been employed and considerable progress has been achieved in recent years [11-15]. For instance, making use of a master oscillator power amplifier (MOPA) laser with high average powers of up to 130 W at sub-ns pulse durations, Legall et al. [15] have described a laser-induced plasma source generated in a liquid nitrogen cryo jet. High quality microscopic images with a resolution of several 10 nm have been presented.

Nevertheless, in order to pave the way for a wider dissemination of lab-scale soft x-ray microscopes there is still the need for further simplification and compaction of these systems. Using laser plasmas generated in short-pulsed gaseous targets enables the construction of long-term stable, clean and compact soft x-ray sources [16, 17], which have already been successfully applied in various fields, ranging from material ablation and structuring [18, 19] to absorption spectroscopy [20] and transmission x-ray microscopy [21, 22]. As the plasma size increases using a gaseous target as alternative to solids or liquid jet target concepts, the photon yield and peak brilliances are smaller. However,

ICXOM23
AIP Conf. Proc. 1764, 030003-1–030003-6; doi: 10.1063/1.4961137
Published by AIP Publishing. 978-0-7354-1422-8/$30.00

the use of cluster beam targets [23], double-stream gas puff targets [24], or the barrel shock approach [25] results in a smaller and brighter plasma due to enhanced particle densities.

In this paper we present an extremely compact, clean and long-term stable soft x-ray microscope operating with monochromatic radiation from He-like nitrogen at a wavelength of 2.88 nm. Along with a description of the setup micrographs from two biological samples are shown.

EXPERIMENTAL

Figure 1 depicts the setup of the table-top soft x-ray microscope consisting basically of a laser-induced plasma source, an ellipsoidal gracing incidence mirror, a Fresnel zone plate objective, and a back-illuminated CCD camera sensitive for soft x-ray radiation.

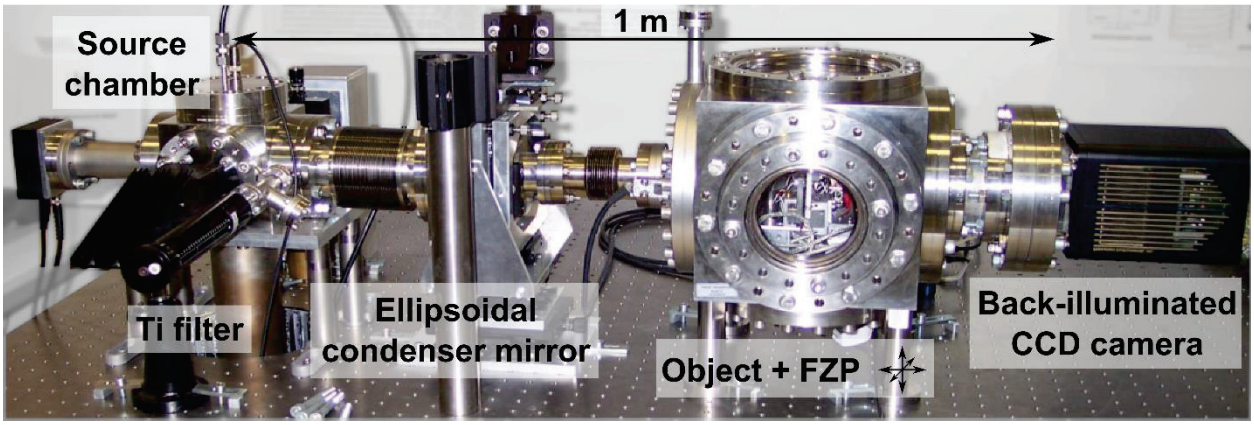

FIGURE 1. Photograph of the table-top soft x-ray microscope (cf. text).

The laser-induced plasma source based on a gas target (nitrogen, gas backing pressure p = 20 bar) and a Nd:YAG laser system (Quantel, wavelength 1064 nm, pulse energy 600 mJ, pulse duration 10 ns, repetition rate 5 Hz) has been described in detail elsewhere [26, 27]. Using a titanium (Ti) filter to block out-of-band radiation (laser radiation, visible light) and radiation below the Ti-edge (λ = 2.7 nm) ensures monochromatic irradiation of the sample at λ = 2.88 nm wavelength (see Fig. 2).

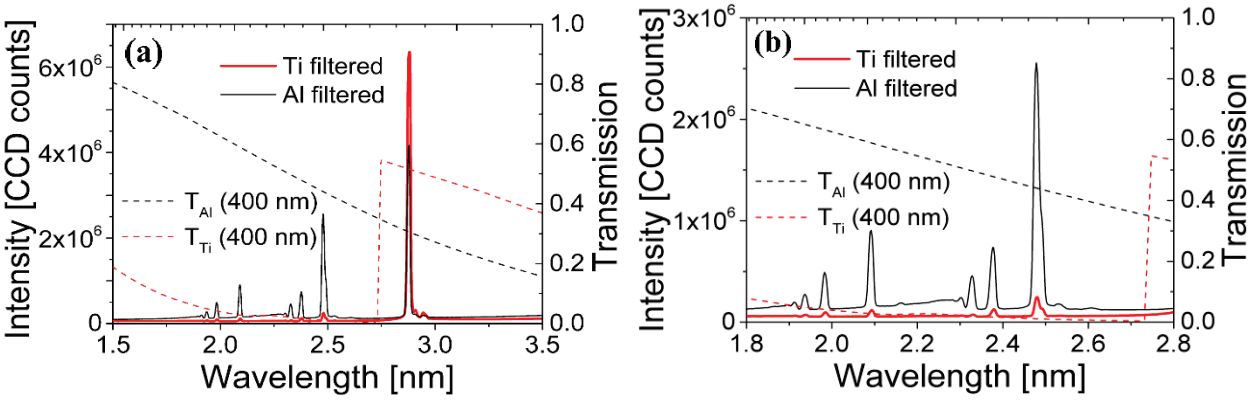

FIGURE 2. Emission spectra of nitrogen in the wavelength range from (a) 1.5 nm to 3.5 nm and (b) 1.8 nm to 2.8 nm measured with Al and Ti filters, respectively. Ti filtering provides monochromatic radiation at λ = 2.88 nm. Transmission data of both filters are taken from CXRO [28].

An ellipsoidal, axisymmetric condenser mirror (Rigaku, Inc., nickel coated, focal length 300 mm, mirror length 100 mm) collects and focusses the soft x-ray radiation from the nitrogen plasma into the object plane. The condenser has an entrance numerical aperture of NA_{C_in} = 0.044 and an exit numerical aperture of NA_{C_out} = 0.071, respectively. A

Gaussian-like spatial profile with a diameter of about 250 µm (FWHM) is registered in the focal plane, utilizing a soft x-ray sensitive, phosphor coated camera (Sony ICX285, 6.45 µm * 6.45 µm pixel size, 1280 * 1024 pixels). The sample is imaged by a Fresnel zone plate objective (ZonePlates Ltd., 120 µm diameter, minimum zone width d_{rn} = 25 nm, number of zones 1200, NA = 0.058) onto a soft x-ray sensitive CCD camera (Roper Scientific, 13 µm * 13 µm pixel size, 1024 * 1024 pixels) using magnifications up to 500x. During image acquisition the CCD camera is cooled down to -40°C to minimize its intrinsic thermal noise.

RESULTS AND DISCUSSION

To assess the imaging performance of the soft x-ray microscope over the full field of view (FOV ≈ 50 µm), initially a featureless "white" field was recorded and then a Siemens star test pattern (NTT-AT, model ATN/XRESO-50, 200 nm Ta on Ru(50 nm)/SiN(200 nm) membrane) was imaged. The corresponding micrograph without sample (see Fig. 3a) indicates an almost uniform illumination over the full FOV (average intensity ≈ 1400 counts per pixel, standard deviation ≈ 100 counts per pixel). Moreover, as seen from Fig. 3b the smallest structures of the Siemens star having a size of 50 nm are resolved in all directions.

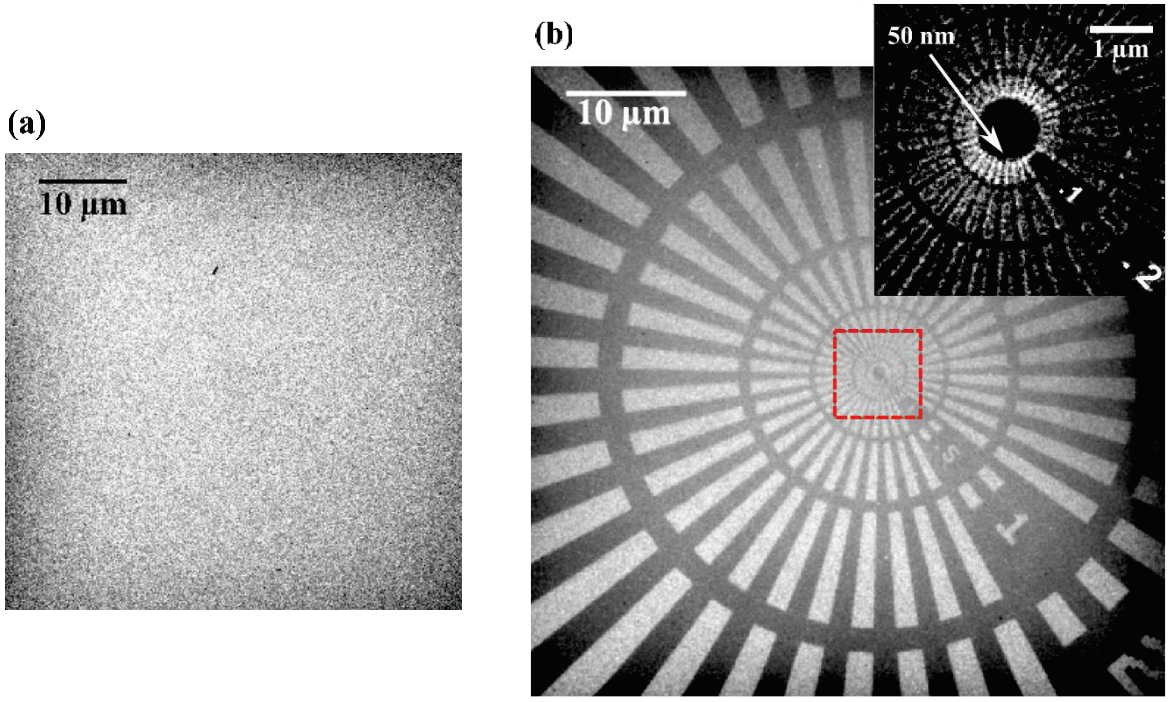

FIGURE 3. Soft x-ray micrograph of (a) featureless "white" field (magnification 250x, effective pixel size 52 nm, 9000 pulses, exposure time 30 min) and (b) Siemens star recorded at λ = 2.88 nm (magnification 250x, effective pixel size 52 nm, 18000 pulses, exposure time 60 min). The inset shows the central part of the Siemens star recorded separately at magnification 500x.

Furthermore, the polyextremophilic bacterium *Deinococcus radiodurans* (DSM No. 20539) and two algae of the genus *Trachelomonas* (*T. oblonga* SAG 1283-11 and *T. hispida* SAG 1283-1) each suspended on a Si_3N_4 membrane (Silson Ltd., thickness 100 nm) were investigated at a magnification of 250x (see Fig. 4 and 5). Although the characteristic shape of *Deinococcus radiodurans* is clearly visible, no internal structure is apparent due to the thickness of the sample and the relatively low brilliance of the plasma. However, there are several options to increase the photon flux of the presented system, which have already been demonstrated in the past. First of all, increased particle densities by the use of either the barrel shock approach [25] or higher gas pressures can improve the brilliance of the plasma by one order of magnitude. In addition, laser systems of higher repetition rate (average power) and/or shorter pulses can be employed. The use of ps laser pulses of the same energy as the currently employed ns pulses can boost the brightness of the laser plasma by a factor of 10 in the "water window" range [29] due to the higher degree of excitation of the gas molecules.

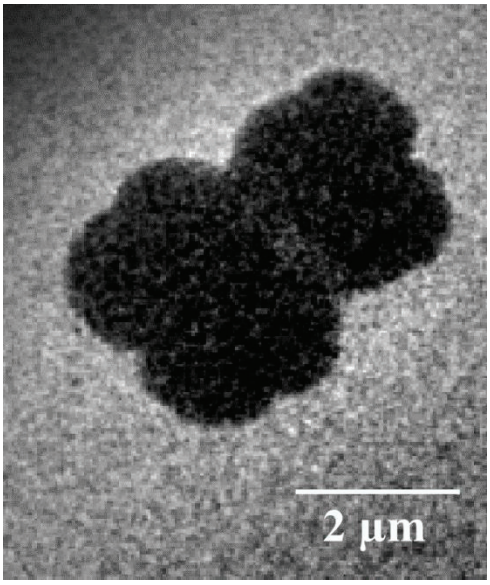

FIGURE 4. Soft x-ray microscopic image of bacterium *Deinococcus radiodurans* (provided by T. Salditt, University of Göttingen) recorded at magnification 250x (effective pixel size 52 nm, 18000 pulses, exposure time 60 min).

In contrast to *Deinococcus radiodurans*, the soft x-ray radiation can penetrate the cell housings of the algal genus *Trachelomonas* (*T. oblonga* and *T. hispida,* see Fig. 5*)*. Moreover, the spherical shape of this shell-like ornamented covering called lorica and the flagellum being characteristic for *Trachelomonas* are clearly imaged**.** Although both biological samples have been exposed to soft x-rays for several hours during the acquisition, radiation damage could be detected neither for the bacterium *Deinococcus radiodurans* nor the algae *Trachelomonas.*

CONCLUSION AND OUTLOOK

In this paper we have presented a table-top soft x-ray microscope operating at 2.88 nm wavelength. It is based on an almost debris-free, long-term stable laser-induced plasma produced in a nitrogen gas. Structures of about 50 nm in size are detectable. Furthermore, applications to biological relevant samples have been demonstrated. However, in order to gain more information on the internal structure of biological objects the brilliance of the source needs to be improved. Various opportunities for scalability of the photon flux have been described and will be incorporated into the system in the future. As a consequence, the exposure times for recording micrographs are reduced and the internal structure of thicker samples can be investigated, thereby maintaining the inherent cleanliness and compactness of the soft x-ray source.

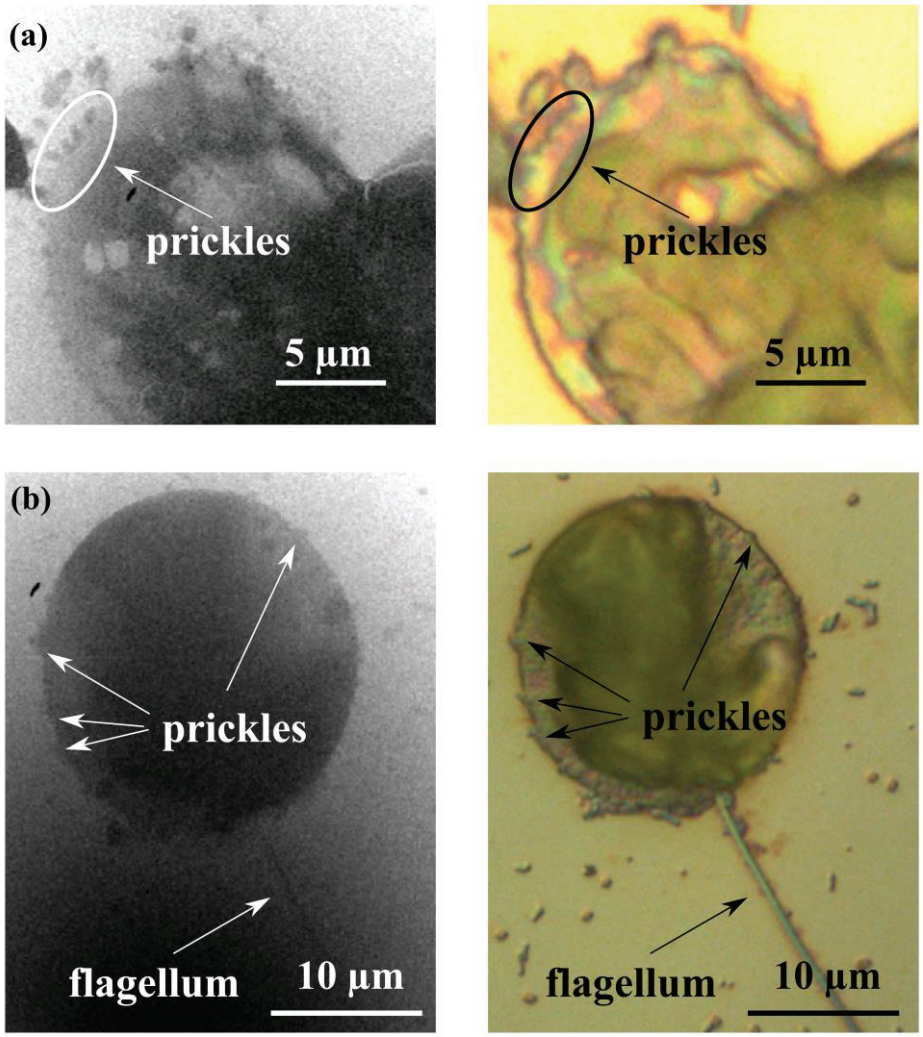

FIGURE 5. (Left) Soft x-ray microscopic image of (a) alga *Trachelomonas oblonga* (SAG 1283-11) and (b) *Trachelomonos hispida* (SAG 1283-1) both recorded at magnification 250x (effective pixel size 52 nm, 18000 pulses, exposure time 60 min). (Right) Corresponding light microscopic images at magnification 100x (Normarski contrast).

ACKNOWLEDGMENTS

Financial support by the "Deutsche Forschungsgemeinschaft" within "Sonderforschungsbereich 755" "Nanoscale Photonic Imaging" (Project C4) is gratefully acknowledged. The authors like to thank T. Salditt (Univ. Göttingen) for providing samples and for stimulating discussions.

REFERENCES

1. W. Meyer-Ilse, D. Hamamoto, A. Nair, S. Levièvre, G. Denbeaux, L. Johnson, A. Pearson, D. Yager, M. Legros, and C. Larabell, J. Microsc. **201**, 395-403 (2000).
2. C. Larabell and M. Le Gros, Mol. Biol. Cell **15**, 957-962 (2004).
3. M. Juenger, V. Lamour, P. Monteiro, E. Gartner, and G. Denbeaux, J. Mater. Sci. Lett. **22**, 1335-1337 (2003).
4. G. Schneider, Ultramicroscopy **75**, 85-104 (1998).

5. D. Weiß, G. Schneider, B. Niemann, P. Guttmann, D. Rudolph, and G. Schmahl, Ultramicroscopy **84**, 185-197 (2000).
6. J. Clowney, M. LeGros, C. Mosley, F. Clowney, E. Markenskoff-Papadimitriou, M. Myllys, G. Barnea, C. Larabell, and S. Lomvardas, Cell **151**, 724-737 (2012).
7. W. Müller, B. Heymann, K. Nagashima, P. Guttmann, S. Werner, S. Rehbein, G. Schneider and J. McNally, J. Struct. Biol. **177**, 179-192 (2012).
8. J. Niclis, S. Murphy, D. Parkinson, A. Zedan, A. Sathananthan, D. Cram, and P. Heraud, J. R. Soc. Interface **12** (2015).
9. S. Myneni, J. Brown, G. Martinez, and W. Meyer-Ilse, Science **286**, 1335-1337 (1999).
10. W. Chao, P. Fischer, T. Tyliszczak, S. Rekawa, E. Anderson, and P. Naulleau, Opt. Express **20**, 9777-9783 (2012).
11. M. Berglund, L. Rymell, M. Peuker, T. Wilhein, and H. Hertz, J. Microsc. **197**, 268-273 (2000).
12. P. Jansson, U. Vogt, and H. Hertz, Rev. Sci. Instrum. **76**, 043503 (2005).
13. P. Takmann, H. Stollberg, G. Johansson, A. Holmberg, M. Lindholm, and H. Hertz, J. Microsc. **226**, 175-181 (2007).
14. M. Benk, K. Bergmann, D. Schäfer, and T. Wilhein, Opt. Lett. **33**, 2359-2361 (2008).
15. H. Legall, G. Blobel H. Stiel, W. Sandner, C. Seim, P. Takman, D. Martz, M. Selin, U. Vogt, H. Hertz, D. Esser, H. Sipma, J. Luttmann, M. Höfer, H. Hoffmann, S. Yulin, T. Feigl, S. Rehbein, P. Guttmann, G. Schneider, U. Wiesemann, M. Wirtz, and W. Diete, Opt. Express **20**, 18362-18369 (2012).
16. H. Fiedorowicz, A. Bartnik, Z. Patron, and P. Piotr, Appl. Phys. Lett. **62**, 2778-2780 (1993).
17. S. Kranzusch and K. Mann, Opt. Commun. **200**, 223-230 (2001).
18. F. Barkusky, C. Peth, A. Bayer, and K. Mann, J. Appl. Phys. **101**, 124908 (2007).
19. A. Bartnik, H. Fiedorowicz, R. Jarocki, J. Kostecki, A. Szczurek, and M. Szczurek, Appl. Phys. B **96**, 727-730 (2009).
20. C. Peth, F. Barkusky, and K. Mann, J. Phys. D: Appl. Phys. **41**, 105202-105207 (2008).
21. M. Müller, T. Mey, J. Niemeyer, and K. Mann, Opt. Express **22**, 23489-23495 (2014).
22. P. Wachulak, A. Torrisi, A. Bartnik, D. Adjei, J. Kostecki, L. Wegrzynski, R. Jarocki, M. Szczurek, H. Fiedorowicz, Appl. Phys. B **118**, 573-578 (2015).
23. G. Kubiak and M. Richardson, US Patent 5,577,092 (1996).
24. H. Fiedorowicz, A. Bartnik, H. Daido, I. Choi, M. Suzuki, and S. Yamagami, Opt. Commun. **184**, 161-167 (2000).
25. T. Mey, M. Rein, P. Großmann, and K. Mann, N. J. Phys. **14**, 073045 (2012).
26. S. Kranzusch, C. Peth, and K. Mann, Rev. Sc. Instrum. **74**, 969-974 (2003).
27. A. Bayer, F. Barkusky, S. Döring, P. Großmann, and K. Mann, X-ray Opt. Instrum. **2010**, 1-9 (2010).
28. B. Henke, E. Gullikson, and J. Davis, Data Tables **54**, 181-342 (1993).
29. M. Müller, F. Kühl, P. Großmann, P. Vrba, and K. Mann, Opt. Express **21**, 12831-12842 (2013).